Evaluation of System Losses for 48V and 380V Solar Powered LVDC Microgrids

Anees, Muhammad; Moaz, Taha; Hussain, Sajid; Khan, Hassan Abbas; Nasir, Mashood

Published in:
2020 IEEE Power and Energy Society General Meeting, PESGM 2020

DOI (link to publication from Publisher):
10.1109/PESGM41954.2020.9281704

Publication date:
2020

Document Version
Accepted author manuscript, peer reviewed version

Evaluation of System Losses for 48V and 380V Solar Powered LVDC Microgrids

Muhammad Anees[1], Taha Moaz, Sajid Hussain and Hassan Abbas Khan[2]
Dept. of Electrical Engineering, SBASSE
Lahore University of Management Sciences (LUMS)
Lahore, Pakistan
muhammad.anees@lums.edu.pk[1], hassan.khan@lums.edu.pk[2]

Mashood Nasir
Dept. of Energy Technology
Aalborg University
9100, Aalborg, Denmark
mnas@et.aau.dk

***Abstract*— International Energy Agency estimates that 1 billion people worldwide have no access to electricity. Commonly prevalent offgrid electrification strategies through a) standalone solar and b) low-power central microgrids are largely suboptimal or prohibitively high cost for services beyond basic electrification (light and mobile phone charging). Distributed solar generation, distributed storage architecture (DGDSA) for DC microgrids with peer-to-peer electricity sharing is now widely reported as the most optimized architecture from systems efficiency perspective with allowance of higher power delivery through resource aggregation. However, DGDSA at distribution voltage of 48V or 380V may have significantly varying efficiencies based on the spatial distribution of village houses for any offgrid electrification scheme. In this work, we evaluate both 380V and 48V distribution for LVDC microgrids incorporating a) converter efficiency and b) distribution efficiency for a typical village deployment in an offgrid scenario. System level efficiency is evaluated for peer to peer power sharing with varying inter-house distance. Results show that for power sharing of 100W, 48V distribution grid is an optimized choice for inter-house distance of up to 100m. For sharing of larger power and higher inter-house distance, 380 V grid becomes a more efficient choice.**

***Index Terms*--DC Microgrid, Efficiency, Grid Voltages, Renewable Energy.**

I. INTRODUCTION

According to the International Energy Agency (IEA) around 1 billion people (i.e. 14% of the world population) do not have access to electricity [1]. It is unlikely that un-electrified population can be given access to electricity through conventional means (utility grid) due to limited power generation, transmission and distribution capacity in many developing regions [2]. Distributed renewable energy resources are being considered as a potential solution to this problem specifically in rural remote areas of South Asia and Sub-Saharan Africa where large offgrid population resides. Fortunately, the available solar potential is very high in these regions (above 6 kWhr/m^2/day for most regions) [3]. Due to this reason, many solar based interventions have taken place in the last few years [4]. Solar home systems have become popular with many interventions in India (Uttar Pradesh electrification [5]), Bangladesh (Grameen Shakti solar solution [6]) and South Africa (Jabula Project [7]) and other countries. However, these systems are largely suboptimal due to limited storage capacity, where surplus power produced by solar is not utilized during day hours when the consumption is typically low. Moreover, studies suggest that these low-power solutions may not be enough for significantly uplifting the socioeconomic status of these communities [8]. This is where sharing of power incorporating usage diversity is key in higher power provisioning to improve socioeconomic standing of remote communities.

AC microgrids are prevalent in many high-end localities, however, they are not readily viable for small offgrid communities [9]. In an offgrid scenario, DC based microgrids are becoming popular due to lower redundant DC-AC-DC conversions [10, 11]. Solar PV based storage assisted DC microgrids are generally considered as a suitable candidate for offgrid electrification. Three major DC microgrid architecture are generally presented and evaluated,

1. Centralized Generation, Centralized Storage Architecture (CGCSA) [12-14].
2. Centralized Generation, Distributed Storage Architecture (CGDSA), [12, 15, 16].
3. Distributed Generation, Distributed Storage Architecture (DGDSA) [17, 18].

In this work, we evaluate DGDSA with regards to peer to peer sharing (not available in the other two architectures due to central generation). This results in higher system scalability and reduces upfront costs with no mandatory requirement of village level electrification up front (details in Section II).

The rest of the paper is summarized as follows: Section II gives an insights into the system architecture of DGDSA microgrid. Section III shows the analysis of the grid interfacing converters and modeling of losses (both conversion and grid distribution). In Section IV, simulated and experimental results are given with conclusions presented in Section V.

II. SYSTEM ARCHITECTURE

A block view of a DGDSA microgrid can be seen in Fig. 1. A nanogrid (NG) is capable of local solar production, storage,

local load management and power sharing to the neighboring nanogrids (NGs). The key feature of DGDSA is power pooling from individual NGs to power up larger community loads (water pumps, schools and basic health units etc.). This architecture is scalable with low upfront infrastructural cost (no requirement of village scale electrification upfront with possibility of adding one house at a time), modular and has the capability of peer to peer power sharing between different households [18]. Each nanogrid consists of the two converters; one for solar power extraction (using MPPT algorithm) and feeding the battery considering the battery state of charge along with load management and second converter for grid interfacing, responsible for the power transactions between grid and battery.

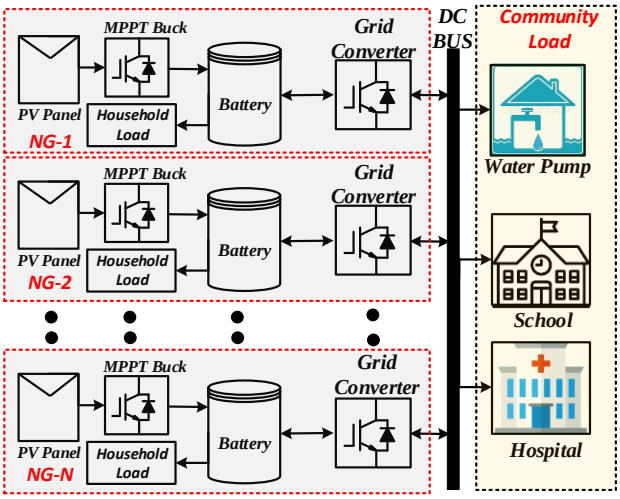

Figure 1. Architecture of DGDSA microgrid with various possible community loads.

The distribution voltage is one of the key design parameters in DGDSA microgrid. It should be optimized based on the amount of power sharing and spatial architecture of a village. Further, the distribution voltages determine the topology and control algorithms for the dc/dc converter, responsible for the grid interface of individual houses (nanogrids). In our previous work [18, 19], the distribution voltages and conductor area are optimized for two DC microgrid connection architecture. However, the previous work did not incorporate converter design as one of the parameters for power sharing aspect. For instance, distributing at lower voltage (48V) will result in higher distribution losses but this will be more cost effective from power conversion perspective due to lower voltage transformations in low power sharing scenarios (a typical case in offgrid communities) and vice versa. Further, the overall system efficiency will also depend on the amount of power sharing as well as spatial arrangement (distance between) of sharing houses. This work, therefore, focuses on this key aspect incorporating both the conversion and distribution losses in a DGDSA microgrid for efficiency evaluation.

Two grid voltage levels are considered for examining the operation of the LVDC DGDSA microgrid i.e., 48V and 380V (two common levels for distribution in DC grids). Distribution losses depend on power transfer level along with conductor resistance and the converter losses depend on power processing as well as converter topology. For 12V (storage level at a NG) to 48V grid voltage bidirectional modified SEPIC-ZETA and Bidirectional modified Boost converter are viable options and their comparison is given in Table I. From the operation of microgrid, storage is the highest cost component in terms of upfront cost and periodic replacements. Therefore, a major deciding factor in selecting a converter is the continuous current operation in the battery among other parameters [20]. Therefore, the bidirectional modified boost converter is selected for the 48 V (DC) distribution microgrid.

TABLE I. GRID INTERFACING CONVERTERS (48V) COMPARISON

Parameters	Bidirectional modified Boost converter		Bidirectional modified SEPIC-ZETA Converter	
Mode	Buck mode (grid to battery)	Boost mode (battery to grid)	SEPIC mode (grid to battery)	ZETA mode (battery to grid)
Input Current	Discont.	Cont.	Cont.	Discont.
Output Current	Cont.	Discont.	Discont.	Cont.
Output Voltage	+ve	+ve	+ve	+ve
No. of high side switches	1		1	

For the converter selection at 380 V microgrid, three bidirectional isolated converters (bidirectional flyback converter, isolated bidirectional Dual Active Bridge (DAB) converter and Isolated Bidirectional Cuk Converter) are evaluated and summarized in Table II. Isolated converters have the advantage of high gains due to transformer action which also isolates nanogrid to microgrid. A major drawback, however, is the increase in conversion losses as well as the cost and weight [21]. Thus, from a systems perspective, by increasing the distribution grid voltage, the distribution line losses decrease but converter losses and cost increase at the same time. The major deciding factor for converter selection is the continuous current into the battery for maximizing battery life. Therefore, bidirectional Cuk converter was chosen for 380V grid implementation. Further, it has the added benefit of having only low sided switches and continuous grid end current which aids to the stability of grid.

TABLE II. GRID INTERFACING CONVERTERS (380V) COMPARISON

Parameters	Isolated Bidirectional Cuk Converter		Isolated Bidirectional DAB converter		Bidirectional Flyback Converter	
	Buck Mode	Boost mode	Buck mode	Boost mode	Buck mode	Boost mode
Input Current	Cont.	Cont.	Discont.	Discont.	Discont.	Discont.
Output Current	Cont.	Cont.	Discont.	Discont.	Discont.	Discont.
Output Voltage	+ve	+ve	+ve	+ve	+ve	+ve
No. of high side switches	0		2		0	

III. MODELING OF CONVERTERS OPERATION AND LOSSES

The selection of converters is dependent on the voltage conversion levels and the models for selected converters are given in this section. Further, losses from distribution perspectives are also discussed in this section.

A. Analysis of Grid Interfacing Converters

1) Modified bidirectional boost converter (12V - 48 V bidirectional)

The modified boost converter is different from the conventional boost converter in a way that the power diode of the conventional boost converter is replaced with an active MOSFET, as shown in Fig. 2.

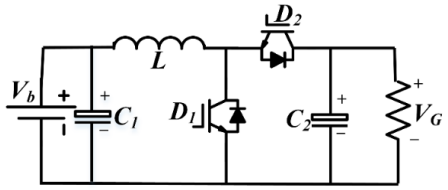

Figure 2. Modified boost converter circuit diagram

There are two modes of operation of the modified boost converter based on the direction of the power flow i.e., boost mode and buck mode. In boost mode, power flows from the battery (12V) to the grid (48V). The duty cycle D_1 controls the output voltage regulation, current regulation as well as power control. Switch 2 remains off ($D_2=0$), and the gain of the converter can be given by (1) [22]. In buck mode, power flows from the grid (48V) to battery (12V). The duty cycle D_2 controls the power flow and regulation while switch 1 remains off ($D_1=0$). The gain of the converter can be given by (2).

$$\frac{V_G}{V_b} = \frac{1}{1-D_1} \tag{1}$$

$$\frac{V_b}{V_G} = D_2 \tag{2}$$

The inductor value is independent of the mode of operation as far as grid voltages and battery voltage stay in steady-state (current design) and inductor current ripple and switching frequency are the same for both modes (Buck and Boost),and the inductor value (L) can be computed by (3) [22, 23]. Capacitor value (C_G) on the grid side is dependent on the value grid voltage and allowable ripple in grid voltage and can be computed by (4) [22]. Similarly, capacitor value on the battery side (C_1) is dependent on the allowable ripple in the battery voltage and is given by (5).

$$L = \frac{V_b \times (V_G - V_b)}{\delta I_L \times F_S \times V_G} \tag{3}$$

$$C_G = \frac{I_{Load(\max)} \times D_1}{F_S \times \delta V_G} \tag{4}$$

$$C_1 = \frac{\delta I_L}{8 \times F_S \times \delta V_b} \tag{5}$$

Where δI_L is the inductor current ripple and F_S is the switching frequency of the converter.

2) Modified bi-directional Cuk converter (12V - 380 V bidirectional)

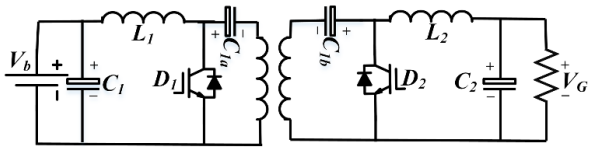

Figure 3. Modified Cuk converter circuit diagram

Conventional Cuk is modified for the bidirectional operation by replacing the power diode by another active switch as shown in the Fig. 3. For the boost mode of operation (power flow from battery to grid), gain of the converter is controlled by D_1 (D_2=0) and is given by (6). Similarly, For the buck mode of operation (power flow from the grid to the battery) D_2 controls the gain and as well as power flow as given by (7) and the switch D_1 remains permanently off ($D_1=0$) [24].

$$\frac{V_G}{V_b} = \frac{nD_1}{1-D_1} \tag{6}$$

$$\frac{V_b}{V_G} = \frac{D_2}{n(1-D_2)} \tag{7}$$

L_1, L_2, C_1, C_2, C_{1a}, and C_{1b} are related inductors and capacitors and their values are dependent on the switching frequency, allowable ripple in input and output currents and voltages. Their calculation criteria is not shown here due to space constraints but verified through hardware testing.

B. Distribution and Conversion Loss Modelling

The main objective of the article is to quantify the tradeoffs between the choice of converters and distribution voltage selection, for a specified power transaction between two nanogrids in a DGDSA microgrid (NG_i and NG_J) separated by a grid length of l_{ij}. There are two types of losses for power transfer from one nanogrid to another nanogrid:

- Conversion losses (depends on the chosen converter topology/voltage conversions and amount of power processing)
- Distribution (I^2R) losses (depending on the distribution conductor length as well the amount of power transferred).

Evaluation of losses gives insights into power transfer efficiencies from one nanogrid (NG_i) to the other (NG_j). Total system loss for the power transfer from i^{th} nanogrid to j^{th} nanogrid (P_{loss}^{ij}) is given by,

$$P_{loss}^{ij} = P_{conv}^{ij} + P_{distr}^{ij} \quad , i \neq j \tag{8}$$

where, P_{conv}^{ij} is conversion losses (battery to grid and vice versa) and P_{distr}^{ij} is distribution losses (between nanogrids) and are given by (9) and (10), respectively.

$$P_{conv} = \left((1-\eta_i^g) * |P_i^g|\right) + \left((1-\eta_j^g) * |P_J^g|\right) \tag{9}$$

$$P_{distr} = \left(\frac{\eta_i^g * P_i^g}{V_i^g}\right)^2 * \left(\frac{R_o}{A}\right) * l_{ij} \tag{10}$$

Where, η_i^g and η_j^g are the conversion efficiencies of converters at i^{th} nanogrid to j^{th} nanogrid. Where P_i^g is the power transfer independent from the direction of flow (measured at battery terminals). V_i^g is the terminal grid voltage at the ith nanogrid, R_o is the resistivity of grid cable and A be the cross-section of cable and l_{ij} is the length of cable connecting i^{th} nanogrid to j^{th} nanogrid.

IV. Experimental Setup and Results

Peer to Peer sharing of up to 100W is evaluated with two other loading levels of sharing at 33% (33W) and 66% (66W). This maximum limit is set to 100W as for vast majority of cases

the power requirement and paying capacity of rural consumers is less than 100W, catering mostly for mobile phone charging, up to 2 fans and a few LEDs [25, 26]. Therefore, for the current setup the converters are rated at this value. This power is delivered from battery of a nanogrid at 12V to 48V and 380V grid through two sets of converters as shown in Fig. 4 and Fig. 5, respectively. The converter efficiencies vary between 94-96% for 48V converter, whereas the 380V converter the efficiency is lower at 84-86% due to higher component count and presence of high frequency transformer. The distribution efficiencies depend on conductor length and resistivity and conductor used for evaluation is taken as 4mm^2. A two nanogrids based microgrid (for both 48V and 380V) is also simulated in eTap software and the layout is shown in Fig. 6 and the converter parameters (for the implemented design) are shown in Table 3.

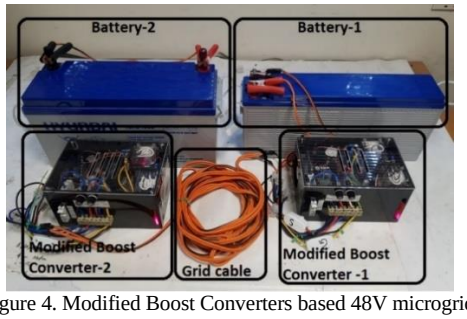

Figure 4. Modified Boost Converters based 48V microgrid.

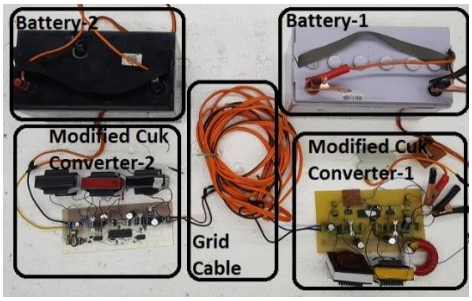

Figure 5. Modified Cuk Converters based 380V microgrid.

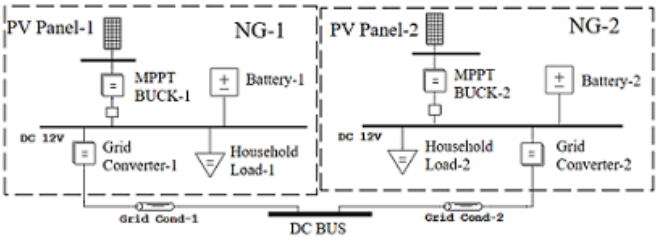

Figure 6. eTap Simulation setup for DGDSA microgrid

System efficiencies (including both conversion and distribution) are computed for 33W, 66W and 100W for end to end power transfer in both simulation and hardware setup and results are shown in Fig. 7. A satisfactory match between measured and the simulated results is observed with less than 5% variation in most cases. For all cases, prototype system efficiencies are slightly lower than the simulation efficiencies which is due to high order parasitic effects in the converters causing additional losses and slightly higher distribution losses in real conductors. Various cases (1-3) are also shown in Fig. 7 which shows the efficiency of the system at various conductor lengths (distance between two nanogrids) for both measured and simulation results.

TABLE III. HARDWARE IMPLEMENTATION PARAMETERS

Parameters	Value(Units)
Modified Cuk Converter (For 12-380 V bidirectional operation)	
Switching frequency	20KHz
Controller	Pic16f877A
IGBTs	FGA25N120
Capacitor (C_1,C_2)	1000uF
Inductors (L_1,L_2)	1.5mH , 70mH
Capacitors (C_{1a}, C_{1b})	100uF
Battery-1 rating	100Ah
Battery-2 rating	100Ah
Modified Boost converters (for 12-48 Vdc bidirectional operation)	
Switching frequency	20KHz
Controller	DsPIC30F4011
Mosfets	IRFB4110
Gate Driver	IR2110
Capacitors (C_1,C_2)	1000uF
Inductor (L)	800mH
Battery-1 rating	100Ah
Battery-2 rating	150Ah
Grid Parameters	
Max Grid Cable length	150 Meters
Max Allowable power transaction	100W
Grid conductor	4mm^2
The resistivity of cable (measured)	0.0048ohms/ft

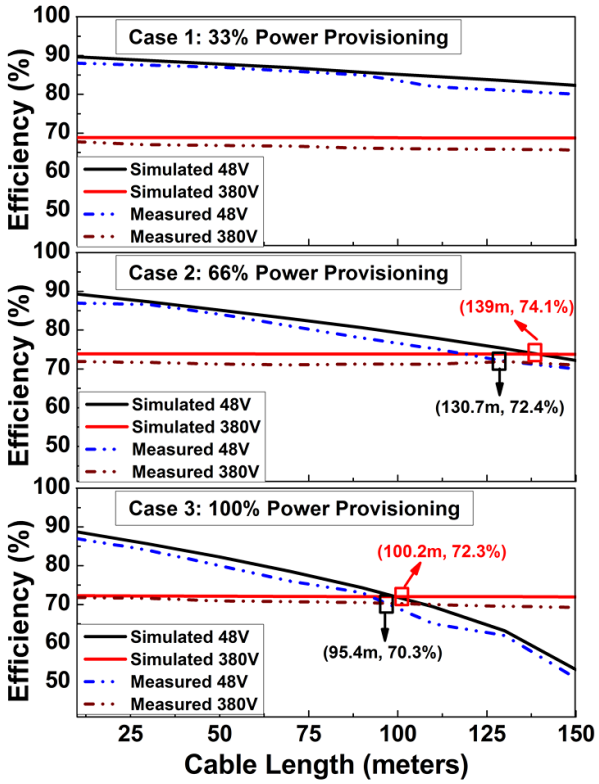

Figure 7. Efficiency variation with conductor length (inter-house) distance variation.

In case 1, 33W power transfer is observed for both 48V and 380V grid systems with conductor lengths varying from 10m to 150m inter-house distance. The system efficiency is higher for 48V grid as converter losses generally dominate which efficiencies for 48V converter significantly higher. For all

conductor lengths (distances between two houses/nanogrids) the 48V microgrid is more efficient. In case 2, when the power transaction is 66W, the end-to-end efficiency varies significantly with distance. Simulation suggests a switchover point between 48V and 380V around 139m (74.1% of system efficiency). Hardware/measured results also show a similar trend with the switch over point to be at 130.7m (72.4% system efficiency). This suggests that for microgrids with distance between nanogrids lower than 130 m, 48 V distribution is more efficient.

In the case of 100W power delivery between nanogrids, the switch over point is 100m for simulation and 95m for measured results. At higher distances, the distribution losses dominate the system efficiency with overall measure efficiency as low as 70.3%. Further, with increase of inter-nanogrid distance the efficiency reduces to 50% for 150m separation. This suggests that for spatially close village structure 48V is a more viable choice for microgrid implementation for power sharing of 100W and vice versa. For higher power sharing, the framework provided in this paper can help to investigate system efficiencies in rural microgrids.

V. Conclusion

This paper evaluates the tradeoff between DGDSA microgrids for the perspective of 48V or 380V distribution grid considering a) the amount of power processing and b) distance between sharing nodes (houses) impacting the efficiency. System efficiency for different levels of power (33W, 66W and 100W) provisioning at 48V and 380V LVDC DGDSA microgrid is simulated and a scaled-down version of DGDSA microgrid is implemented using bidirectional isolated boost (for 48V grid) and modified Cuk (for 380V grid), respectively. Results show that 48V system has lower conversion losses but higher distribution losses. In contrast, 380 V system is generally less efficient in power processing but due to high voltage transformation but the distribution loss is negligible at these power levels. For a typical offgrid scenario with target power sharing of up to 100W, 48V microgrid is more viable with end-to-end efficiency of up to 88% with 10m distance.

This work gives insights into efficiency improvements in peer to peer sharing based microgrids with central idea of power sharing and aggregation to lower the costs and enhance the financial sustainability of these systems where consumers can generate revenue by sharing power when available or in predefined settings.

Acknowledgment

Authors acknowledge Higher Education Commission HEC, Pakistan, for their financial support for this work through grant TDF03-171.

References

[1] International Energy Agency. (4 Nov,2019). Energy Access Outlook.

[2] UN News. (4 Nov, 2019). UN projects world population to reach 8.5 billion by 2030, driven by growth in developing countries. Available: https://news.un.org/en/story/2015/07/505352-un-projects-world-population-reach-85-billion-2030-driven-growth-developing

[3] M. Nasir, M. Anees, H. A. Khan, I. Khan, Y. Xu, and J. M. Guerrero, "Integration and Decentralized Control of Standalone Solar Home Systems for off-grid Community Applications," IEEE Transactions on Industry Applications, 2019.

[4] M. Nasir, H. A. Khan, K. A. K. Niazi, Z. Jin, and J. M. Guerrero, "Dual-loop control strategy applied to PV/battery-based islanded DC microgrids for swarm electrification of developing regions," The Journal of Engineering, vol. 2019, pp. 5298-5302, 2019.

[5] The World Bank. Electricity production from renewable sources, excluding hydroelectric (kWh) - India, Sub-Saharan Africa. Available: https://data.worldbank.org/indicator/EG.ELC.RNWX.KH?locations=IN-ZG

[6] J. Urpelainen, "Energy poverty and perceptions of solar power in marginalized communities: Survey evidence from Uttar Pradesh, India," Renewable Energy, vol. 85, pp. 534-539, 2016.

[7] Newcombe and E. K. Ackom, "Sustainable solar home systems model: Applying lessons from Bangladesh to Myanmar's rural poor," Energy for Sustainable Development, vol. 38, pp. 21-33, 2017.

[8] Zonke Energy. (4 Nov, 2019). SERVICING OFF-GRID COMMUNITIES WITH RENEWABLE ENERGY. Available: http://www.zonkeenergy.com/JabulaProject.php

[9] S. BHATTACHARYA and R. AGARWAL, "ANALYSIS OF SOCIO-ECONOMIC BENEFIT OF ELECTRIFICATION THROUGH CREDA IN CHHATTISGARH STATE," CLEAR International Journal of Research in Commerce & Management, vol. 7, 2016.

[10] S. Dhundhara, Y. P. Verma, and A. Williams, "Techno-Economic Evaluation of AC and DC Microgrid Systems," in Applications of Computing, Automation and Wireless Systems in Electrical Engineering, ed: Springer, 2019, pp. 265-280.

[11] R. Zhang and B. Hredzak, "Nonlinear Sliding Mode and Distributed Control of Battery Energy Storage and Photovoltaic Systems in AC Microgrids with Time Delays," IEEE Transactions on Industrial Informatics, 2019.

[12] L. E. Zubieta, "Are microgrids the future of energy?: Dc microgrids from concept to demonstration to deployment," IEEE Electrification Magazine, vol. 4, pp. 37-44, 2016.

[13] P. A. Madduri, J. Poon, J. Rosa, M. Podolsky, E. A. Brewer, and S. R. Sanders, "Scalable DC microgrids for rural electrification in emerging regions," IEEE Journal of Emerging and Selected Topics in Power Electronics, vol. 4, pp. 1195-1205, 2016.

[14] P. Loomba, S. Asgotraa, and R. Podmore, "DC solar microgrids—A successful technology for rural sustainable development," in 2016 IEEE PES PowerAfrica, 2016, pp. 204-208.

[15] M. Nasir, S. Iqbal, and H. A. Khan, "Optimal Planning and Design of Low-Voltage Low-Power Solar DC Microgrids," IEEE Transactions on Power Systems, vol. 33, pp. 2919-2928, 2018.

[16] M. Balijepalli, S. Khaparde, and C. Dobariya, "Deployment of microgrids in India," in IEEE PES General Meeting, 2010, pp. 1-7.

[17] P. A. Madduri, J. Rosa, S. R. Sanders, E. A. Brewer, and M. Podolsky, "Design and verification of smart and scalable DC microgrids for emerging regions," in 2013 IEEE Energy Conversion Congress and Exposition, 2013, pp. 73-79.

[18] M. Nasir, N. A. Zaffar, and H. A. Khan, "Analysis on central and distributed architectures of solar powered DC microgrids," in 2016 Clemson University Power Systems Conference (PSC), 2016, pp. 1-6.

[19] M. Nasir, H. A. Khan, A. Hussain, L. Mateen, and N. A. Zaffar, "Solar PV-Based Scalable DC Microgrid for Rural Electrification in Developing Regions," IEEE Transactions on Sustainable Energy, vol. 9, pp. 390-399, 2018.

[20] M. Hamza, M. Shehroz, S. Fazal, M. Nasir, and H. A. Khan, "Design and analysis of solar PV based low-power low-voltage DC microgrid architectures for rural electrification," in 2017 IEEE Power & Energy Society General Meeting, 2017, pp. 1-5.

[21] M. Faisal, M. A. Hannan, P. J. Ker, A. Hussain, M. B. Mansor, and F. Blaabjerg, "Review of energy storage system technologies in microgrid applications: Issues and challenges," Ieee Access, vol. 6, pp. 35143-35164, 2018.

[22] B. Sri Revathi, M. Prabhakar, and F. Gonzalez-Longatt, "High-gain–high-power (HGHP) DC-DC converter for DC microgrid applications: Design and testing," International Transactions on Electrical Energy Systems, vol. 28, p. e2487, 2018.

[23] Texas Instruments. (4 Nov, 2019). Basic Calculation of a Boost Converter's Power Stage. Available: http://www.ti.com/lit/an/slva372c/slva372c.pdf
[24] Texas Instruments. (4 Nov, 2019). Basic Calculation of a Buck Converter's Power Stage. Available: http://www.ti.com/lit/an/slva477b/slva477b.pdf
[25] F. Galea, M. Apap, C. S. Staines, and J. Cilia, "Design of a high efficiency wide input range isolated Ćuk Dc-Dc converter for grid connected regenerative active loads," 2011.
[26] H. A. Khan, H. F. Ahmad, M. Nasir, M. F. Nadeem, and N. A. Zaffar, "Decentralised electric power delivery for rural electrification in Pakistan," Energy Policy, vol. 120, pp. 312-323, 2018/09/01/ 2018.
[27] S. Numminen, S. Yoon, J. Urpelainen, and P. Lund, "An evaluation of dynamic electricity pricing for solar micro-grids in rural India," Energy strategy reviews, vol. 21, pp. 130-136, 2018.